

# Structure determination and by-product profile of the NK<sub>2</sub> receptor antagonist nepadutant, a bicyclic glycopeptide

Hardy Weißhoff<sup>a</sup>, Thomas Nagel<sup>b</sup>, Andre Hänsicke<sup>b</sup>, Adolf Zschunke<sup>a</sup>, Clemens Mügge<sup>a,\*</sup>

<sup>a</sup>*Institute of Chemistry, Humboldt University of Berlin, Hessische Str. 1-2, D-10115 Berlin, Germany*

<sup>b</sup>*Berlin-Chemie AG, Department of Chemistry, Glienicker Weg 125, 12489 Berlin, Germany*

Received 15 December 2000; revised 29 January 2001; accepted 1 February 2001

First published online 14 February 2001

Edited by Hans Eklund

**Abstract** We have synthesized and fully characterized the NK<sub>2</sub> receptor antagonist nepadutant and its by-products using nuclear magnetic resonance (NMR) and restrained molecular dynamics. The agent consists of an active bicyclic hexapeptide combined with a sugar residue. Analysis of the high-performance liquid chromatogram and the mass spectroscopy spectra yields traces of three by-products with the same molecular weight as the main product. The conformation of the molecules in the bicyclic hexapeptide segment, the active region, is well defined, whereas the sugar moiety is disordered. For the peptide region of nepadutant and all of its by-products, the NMR observables can be described by a single backbone conformation, more specifically a  $\beta$ I,  $\beta$ II-turn arrangement. The active dipeptide unit Trp-Phe occupies the *i*+1 and *i*+2 position of a  $\beta$ I-turn. The by-product profile is characterized by different forms of sugars which are caused mainly by isomerization in the process of ring opening. © 2001 Federation of European Biochemical Societies. Published by Elsevier Science B.V. All rights reserved.

**Key words:** Cyclic glycopeptide; Nuclear magnetic resonance; Turn; Tachykinin receptor antagonist; Mutarotation

## 1. Introduction

Tachykinins are a family of neuropeptides widely distributed in the mammalian central and peripheral nervous systems, which produce a wide range of biological effects through the stimulation of three distinct receptor subtypes NK<sub>1</sub> to NK<sub>3</sub> [1]. Among the three natural mammalian tachykinins, substance P displays the highest affinity for the NK<sub>1</sub> receptor, Neurokinin A for the NK<sub>2</sub> receptor and Neurokinin B for the

NK<sub>3</sub> receptor. Neurokinin A has links to chronic diseases in the gastrointestinal, respiratory and genitourinary tracts [2]. The development of novel drugs based on peptide and non-peptide antagonists of the NK<sub>2</sub> receptor may provide new opportunities for the therapy of diseases like asthma, inflammatory bowel disorders, rheumatoid arthritis, pain and psychiatric disorders [3].

The development of peptide-based NK<sub>2</sub> receptor antagonists proceeded starting from Neurokinin A via linear peptides, monocyclic pseudopeptides extending to bicyclic peptides [4–7]. The bicyclic glyco-hexapeptide nepadutant, cyclo{[Asn( $\beta$ -D-GlcNAc)-Asp-Trp-Phe-2,3-diamino propionic acid (Dpr)-Leu] cyclo(2 $\beta$ -5 $\beta$ )}, is such an effective and selective tachykinin NK<sub>2</sub> receptor antagonist. The pharmacological profile of nepadutant has been the subject of extensive research [8,9]. It was found that nepadutant showed negligible binding affinity at 50 different receptors, including tachykinin NK<sub>1</sub> and NK<sub>3</sub> receptors and ion channels. Otherwise, nepadutant competitively binds with high affinity to the human NK<sub>2</sub> receptor, displacing radiolabelled [<sup>125</sup>I]-Neurokinin A. Therefore, it is a suitable candidate for clinical testing in humans, especially for studying the pathophysiological significance of tachykinin NK<sub>2</sub> receptors. Defacto, nepadutant is currently in phase II clinical trials and was selected as reference compound for further developments.

Nepadutant is a glycosylated analogue of the potent, selective, conformationally constrained NK<sub>2</sub> receptor antagonist MEN10627 (cyclo{[Met-Asp-Trp-Phe-Dpr-Leu] cyclo(2 $\beta$ -5 $\beta$ )}) [6,7]. The introduction of the sugar moiety did not produce major changes in the affinity profile of this antagonist as compared to MEN10627, but markedly improved its *in vivo* potency and duration of action [10]. The by-product profile of nepadutant after final purification is reproducibly characterized by the presence of three by-products MEN11420A (cyclo{[Asn(2-acetamido-2-deoxy- $\beta$ -D-mannopyranose)-Asp-Trp-Phe-Dpr-Leu] cyclo(2 $\beta$ -5 $\beta$ )}), MEN11420C (cyclo{[Asn(2-acetamido-2-deoxy- $\beta$ -D-glucopyranose)-Asp-Trp-Phe-Dpr-Leu] cyclo(2 $\beta$ -5 $\beta$ )}) and MEN11420D (cyclo{[Asn(2-acetamido-2-deoxy- $\alpha$ -D-glucopyranose)-Asp-Trp-Phe-Dpr-Leu] cyclo(2 $\beta$ -5 $\beta$ )}) in a range between 0.1 and 1.5%. Our aim was the complete solution structure elucidation of nepadutant and mainly of its by-products for qualification as a new drug substance. The structure determination by combined nuclear magnetic resonance (NMR) spectroscopy and restraint molecular dynamics calculations is described. A detailed insight into the 3D structures of the synthetic tachykinin NK<sub>2</sub> receptor antagonist, nepadutant, and the attendant unavoidable by-products, is given.

\*Corresponding author. Fax: (49)-30-20937561.  
E-mail: muegge@chemie.hu-berlin.de

**Abbreviations:** Nepadutant (MEN11420), cyclo{[Asn(2-acetamido-2-deoxy- $\beta$ -D-glucopyranose)-Asp-Trp-Phe-Dpr-Leu] cyclo(2 $\beta$ -5 $\beta$ )}; MEN11420A, cyclo{[Asn(2-acetamido-2-deoxy- $\beta$ -D-mannopyranose)-Asp-Trp-Phe-Dpr-Leu] cyclo(2 $\beta$ -5 $\beta$ )}; MEN11420C, cyclo{[Asn(2-acetamido-2-deoxy- $\beta$ -D-glucopyranose)-Asp-Trp-Phe-Dpr-Leu] cyclo(2 $\beta$ -5 $\beta$ )}; MEN11420D, cyclo{[Asn(2-acetamido-2-deoxy- $\alpha$ -D-glucopyranose)-Asp-Trp-Phe-Dpr-Leu] cyclo(2 $\beta$ -5 $\beta$ )}; MEN10627, cyclo{[Met-Asp-Trp-Phe-Dpr-Leu] cyclo(2 $\beta$ -5 $\beta$ )}; MEN11282, cyclo{[Asp-Asp-Trp-Phe-Dpr-Leu] cyclo(2 $\beta$ -5 $\beta$ )}; MEN11295, cyclo{[Asn-Asp-Trp-Phe-Dpr-Leu] cyclo(2 $\beta$ -5 $\beta$ )};  $\beta$ -D-GlcNAc, 2-acetamido-2-deoxy- $\beta$ -D-glucopyranose; Dpr, 2,3-diamino propionic acid

## 2. Materials and methods

### 2.1. Synthesis and isolation

Nepadutant was synthesized by the coupling of the peptide precursor MEN11282 (cyclo{(Asp-Asp-Trp-Phe-Dpr-Leu) cyclo(2 $\beta$ -5 $\beta$ )}) with  $\beta$ -D-2-acetamido-2-deoxy-glucopyranosylamine. MEN11282 was synthesized by classical peptide synthesis procedures in solution using the *tert*-butoxycarbonyl (Boc), benzyloxycarbonyl- (Z) groups for N-terminal and the methyl ester group (OMe) for the C-terminal protection.

The main and minor components of nepadutant were isolated by reversed phase HPLC procedures in acetonitrile/water systems [11]. The by-products of nepadutant could be isolated with a purity of 98.8% MEN11420A, 84.6% MEN11420C and 89.6% MEN11420D for structure elucidation. The identity of the isolated samples was proved by analytical HPLC of MEN11420 with spiked amounts of the isolates. Mass spectrometric analyses were performed on a VG Quattro mass spectrometer (Altrincham, UK) equipped with standard electrospray (ES) ion source.

### 2.2. NMR spectroscopy

Samples for NMR spectroscopy were prepared by dissolving 5 mg of the reference compound nepadutant and 1–2 mg of isolated MEN11420A, MEN11420C and MEN11420D in 0.75 ml of DMSO- $d_6$  in a 5 mm sample tube (Wilmad, NJ, USA).

2D spectra were recorded at 600 MHz on a Bruker AMX 600 spectrometer with a spectral width of 7250 Hz for protons in both dimensions. Data matrices typically consisted of 2048 complex points in F2 for each of the 512 F1 increments, the data being zero-filled to a 2048  $\times$  1024 complex matrix before transformation. The apodization functions used in processing were 90° shifted sine-bell squared for all 2D experiments. The spectra were processed using the XWINNMR program (Bruker, Germany) on a Silicon Graphics O2 workstation. ROESY crosspeaks were integrated by the AURELIA software (Bruker, Germany) including offset correction according to Bull [12]. Chemical shifts and coupling constants were evaluated from complete simulation of  $^1\text{H}$ -NMR spectra with WIN-DAISY (Bruker-Franzen, Germany). Selected parameters for 2D-NMR experiments: TOCSY, mixing time 20 and 70 ms, NS = 16–40; ROESY, mixing time 120, 150, 180 ms, NS = 64–80; NOESY, mixing time 50, 120, 200, 400 ms, NS = 40–80.

### 2.3. Molecular modelling

The data derived from NMR spectra were analyzed via *in vacuo* restrained molecular dynamics simulations (rMD) on an IRIS Indigo computer using XPLOR [13]. At first 50 starting structures were initially generated by randomizing the atom coordinates of a manually constructed structure followed by energy minimization and rMD at 300 K. The L-configuration of the amino acids Leu, Phe and Asp is confirmed by racemization investigations of nepadutant and MEN11420A–D. In order to find starting conformations reflecting as much as possible the restrained geometry, we applied another run with a strong force constant  $k(\text{NOE}) = 50.0 \text{ kcal}/(\text{mol } \text{\AA}^2)$ .

All structures were subjected to a subsequent rMD protocol in conjunction with a simulated annealing procedure. We carried out an rMD simulation at 1000 K under non-bound conditions followed by cooling to 100 K. The seven structures with the lowest total energy were then used for an additional rMD simulation over 90 ps at 300 K. All force constants were set to 1. The structures were finally relaxed with an energy minimization.

## 3. Results

### 3.1. By-product profile

The by-product profile of the crude peptide nepadutant before final purification is reproducible characterized by the presence of the impurities MEN11282 and MEN11295 (cyclo{(Asn-Asp-Trp-Phe-Dpr-Leu) cyclo(2 $\beta$ -5 $\beta$ )}) known to be induced by the way of syntheses in a range up to 3% and the by-products MEN11420A, MEN11420C and MEN11420D in a range between 0.1 and 1.5%. MEN11282 is the starting material of the last coupling step and MEN11295 is a by-

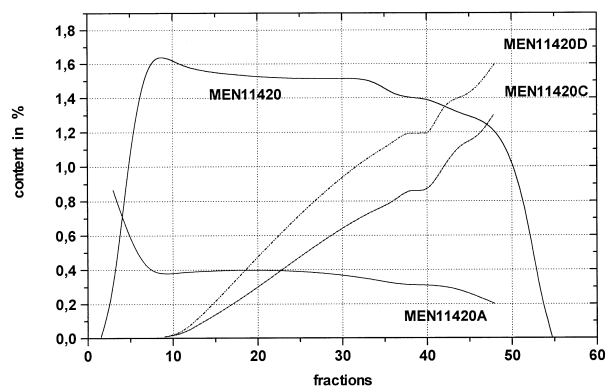


Fig. 1. Distribution of nepadutant (MEN11420) and its by-products in the preparative RP-18 chromatography.

product of the last coupling step. Both impurities can be quantitatively separated by the final purification.

After the final purification, beside the desired compound also the by-products MEN11420A, MEN11420C and MEN11420D are present in all batches of nepadutant with values of up to 0.8, 1.0 and 1.5%, respectively. The analysis of the distribution of these by-products in the fractions of the final preparative HPLC purification demonstrates the impossibility of their quantitative separation (Fig. 1). Nevertheless, the distribution of the mentioned by-products in the main peak of the nepadutant purification indicates an enrichment of the by-product MEN11420A in the pre-fractions and of the by-products MEN11420C and MEN11420D in the post-fractions. Further accumulation of those materials by repeated re-chromatography was expected to provide the pure by-products for structure elucidation. This procedure permits us to carry out a detailed conformational analysis for all four compounds.

### 3.2. Structural characterization

The bicyclic NK<sub>2</sub> receptor antagonist nepadutant consists of two characteristic structure units of different chemical nature. These are the peptidic moiety containing the pharmacologically active amino acid sequence and the solubility-increasing carbohydrate moiety.

Mass spectra were measured for all four compounds. Interestingly, the molecular mass of the three by-products and of nepadutant was determined to be (MH<sup>+</sup>) at *m/z* 947. The mass spectra show practically identical fragmentation patterns. The MS/MS spectrum of *m/z* 947 gives the ion at *m/z* 727, corresponding to the peptide core and the ion at *m/z* 204 corresponding to the sugar moiety. It was found that the MS, MS/MS and MS<sup>3</sup> spectra of the by-products are almost superimposable to that of nepadutant. The most relevant differences were found in the MS/MS spectra of the ion *m/z* 204, in which the masses of the fragments are the same, but their relative abundances vary slightly. This reinforces our hypothesis, that the structural differences between nepadutant and its by-products are located in the sugar moiety.

### 3.3. Structural analysis of the peptide moiety

Evaluation of the NOESY/ROESY spectra and coupling constants of the four compounds, resulted in very similar spectral information. It is clear evidence for the close relationship of the peptide conformations between nepadutant and its

Table 1

<sup>1</sup>H-NMR chemical shifts, coupling constants and  $\Delta\delta/\Delta T$  values for the peptide moiety of nepadutant, as well as chemical shifts and coupling constants for the sugar moieties of nepadutant and the by-products in DMSO-d<sub>6</sub>

Nepadutant amino acid (333 K)	$\delta_{\text{NH}}$ (ppm)	$\delta_{\text{H}\alpha}$ (ppm)	$\delta_{\text{H}\beta'}$ (ppm)	$\delta_{\text{H}\beta}$ (ppm)	$^3J_{\text{NH}\alpha}$ (Hz)	$^3J_{\text{H}\alpha\text{H}\beta'}$ (Hz)	$^3J_{\text{H}\alpha\text{H}\beta}$ (Hz)	$\Delta\delta/\Delta T$ (ppb K <sup>-1</sup> )
Asn <sup>1</sup>	8.81	4.36	2.94	2.21	6.4	6.0	5.9	4.8
Asp <sup>2</sup>	7.26	4.55	2.87 <sup>(S)</sup>	2.65 <sup>(R)</sup>	6.8	4.2	4.1	0.3
Trp <sup>3</sup>	8.58	4.17	2.87 <sup>(S)</sup>	2.74 <sup>(R)</sup>	3.8	9.5	4.2	5.3
Phe <sup>4</sup>	7.99	4.47	3.29 <sup>(S)</sup>	2.60 <sup>(R)</sup>	7.7	5.6	8.8	1.2
Dpr <sup>5</sup>	6.99	4.43	3.97 <sup>(S)</sup>	3.54 <sup>(R)</sup>	6.5	2.4	2.4	0.4
Leu <sup>6</sup>	8.35	4.09	1.52 <sup>(S)</sup>	1.40 <sup>(R)</sup>	5.0	8.9	5.5	4.4
Sugar moiety (298 K)	$\delta_{\text{C1H}}$ $\delta_{\text{C6H}}$	$\delta_{\text{C2H}}$ $\delta_{\text{O3H}}$	$\delta_{\text{C3H}}$ $\delta_{\text{O4/5H}}$	$\delta_{\text{C4H}}$ $\delta_{\text{O6H}}$	$\delta_{\text{C5H}}$ $\delta_{\text{N1H}}$	$\delta_{\text{C6H}}$ $\delta_{\text{N2H}}$	$^3J_{\text{N1H-C1H}}$ $^3J_{\text{C1H-C2H}}$	$^3J_{\text{N2H-C2H}}$ $^3J_{\text{C2H-C3H}}$
Nepadutant	4.81 3.65	3.50 4.94	3.28 4.98	3.04 4.51	3.06 8.09	3.42 7.75	9.0 9.4	8.9 9.6
MEN11420A	5.02 3.65	4.07 4.77	3.46 4.79	3.29 4.35	3.09 8.05	3.48 7.15	8.9 1.2	9.5 4.4
MEN11420C	5.26 3.55	3.87 5.20	3.89 4.61	3.62 4.41	3.72 8.22	3.35 8.18	9.1 3.1	7.3 n.d.
MEN11420D	5.35 3.52	3.78 4.83	3.57 5.06	3.19 4.42	3.35 8.30	3.47 7.09	9.3 4.9	8.8 11.0

n.d. = not determined.

by-products. Therefore, we will only discuss the conformational analysis of nepadutant and MEN11420D, the most predominant by-product.

The <sup>1</sup>H-NMR spectra of nepadutant and MEN11420D show only one set of resonances with very broad resonance lines for three amino acid residues at 298 K. Changing measurement conditions, especially the raise of the temperature to 333 K leads to spectra with shape lines and well resolved NH resonances. The results of the chemical shift assignments and coupling constants for the peptide moieties are shown in Table 1.

The temperature coefficients of the NH chemical shifts are in both cases very small for amino acids Asp<sup>2</sup> and Dpr<sup>5</sup>, pointing to the involvement of Asp<sup>2</sup>NH and Dpr<sup>5</sup>NH in a hydrogen bond. With regard to the structure of other cyclic hexapeptides, we could expect a peptide conformation with two  $\beta$ -turns each stabilized by a CO<sup>(i)</sup> → NH<sup>(i+3)</sup> hydrogen bond [14]. Here, Asp<sup>2</sup> and Dpr<sup>5</sup> act as hydrogen bond donors as well as acceptors, resulting in the hydrogen bonds Asp<sup>2</sup>CO → Dpr<sup>5</sup>NH and Dpr<sup>5</sup>CO → Asp<sup>2</sup>NH. We additionally observed a small temperature coefficient for Phe<sup>4</sup>NH, which can be explained by an interaction between Phe<sup>4</sup>NH with the rigid side chain carbonyl function of Asp<sup>2</sup>, involved in the side chain linkage.

The medium range NOEs (Table 2) and dihedrals  $\phi$  derived from the  $^3J_{\text{NH}\alpha}$  and  $^3J_{\text{NH}\beta}$  coupling constants were used as inputs for the rMD calculations.  $^3J_{\text{NH}\beta}$  coupling constants were measured only for nepadutant because of the high concentrations necessary for the HETLOC experiment [15]. The NH-H $\beta$  crosspeaks of Trp<sup>3</sup> and Leu<sup>6</sup> show valuable coupling patterns for the determination of  $^3J_{\text{NH}\beta}$  coupling constants, 2.0 Hz for Trp<sup>3</sup> and 2.6 Hz for Leu<sup>6</sup>.

The results obtained by the MD refinement of the peptide moiety of nepadutant and its by-products revealed a double  $\beta$ -turn arrangement with Trp and Leu in position *i*+1 of a standard turn structure. Specifically, a  $\beta$ I-turn in the Asp-Trp-Phe-Dpr and a  $\beta$ II-turn in the Dpr-Leu-Asn-Asp regions were observed. The final seven lowest energy structures belong to one conformational family (Fig. 2). These structures all converged to a similar backbone-fold within the range of 12 kJ mol<sup>-1</sup>. Further restriction of the cyclic peptide backbone through the additional side chain-side chain linkage probably produces a very stable conformation and causes only few fluctuations during the molecular dynamic simulation. Approximately 85% of the conformations of the last 30 ps trajectories show the typical hydrogen pattern of a double  $\beta$ -turn arrangement.

The arrangement of the Trp<sup>3</sup> and Phe<sup>4</sup> side chains is notice-

Table 2

Comparison of the experimental (NOESY) and calculated (rMD) backbone interproton distances of nepadutant

Proton pair		$r^{\text{NOE}}$	$r^{\text{MD}}$	Proton pair		$r^{\text{NOE}}$	$r^{\text{MD}}$
Asn <sup>1</sup> NH	Asp <sup>2</sup> NH	2.5	2.61	Asp <sup>2</sup> NH	Asp <sup>2</sup> Hβ <sup>(R)</sup>	2.9	3.05
Asp <sup>2</sup> NH	Dpr <sup>5</sup> NH	3.2	3.50	Trp <sup>3</sup> NH	Asp <sup>2</sup> Hβ <sup>(S)</sup>	3.0	2.87
Asp <sup>2</sup> NH	Dpr <sup>5</sup> SCNH	3.3	3.19	Trp <sup>3</sup> NH	Trp <sup>3</sup> Hβ <sup>(S)</sup>	2.8	3.00
Trp <sup>3</sup> NH	Phe <sup>4</sup> NH	3.7	3.12	Trp <sup>3</sup> NH	Trp <sup>3</sup> Hβ <sup>(R)</sup>	2.4	2.35
Phe <sup>4</sup> NH	Dpr <sup>5</sup> NH	2.8	2.85	Phe <sup>4</sup> NH	Trp <sup>3</sup> Hβ <sup>(S)</sup>	2.5	2.35
Dpr <sup>5</sup> NH	Dpr <sup>5</sup> SCNH	n.d.	3.73	Phe <sup>4</sup> NH	Phe <sup>4</sup> Hβ <sup>(R)</sup>	2.6	2.69
Leu <sup>6</sup> NH	Dpr <sup>5</sup> SCNH	2.3	2.45	Phe <sup>4</sup> NH	Phe <sup>4</sup> Hβ <sup>(S)</sup>	3.4	3.74
				Dpr <sup>5</sup> SCNH	Dpr <sup>5</sup> Hβ <sup>(R)</sup>	2.7	2.71
Asn <sup>1</sup> NH	Leu <sup>6</sup> Hα	2.3	2.19	Dpr <sup>5</sup> SCNH	Dpr <sup>5</sup> Hβ <sup>(S)</sup>	2.7	2.94
Asp <sup>2</sup> NH	Leu <sup>6</sup> Hα	3.8	3.34	Dpr <sup>5</sup> SCNH	Dpr <sup>5</sup> Hβ <sup>(R)</sup>	2.4	2.29
Trp <sup>3</sup> NH	Asp <sup>2</sup> Hα	2.1	2.36	Leu <sup>6</sup> NH	Dpr <sup>5</sup> Hβ <sup>(R)</sup>	2.3	1.95
Phe <sup>4</sup> NH	Trp <sup>3</sup> Hα	3.2	3.60	Leu <sup>6</sup> NH	Dpr <sup>5</sup> Hβ <sup>(S)</sup>	3.5	3.49
Dpr <sup>5</sup> NH	Phe <sup>3</sup> Hα	2.8	3.02	Leu <sup>6</sup> NH	Leu <sup>6</sup> Hβ <sup>(S)</sup>	2.4	2.49
Leu <sup>6</sup> NH	Dpr <sup>5</sup> Hα	2.6	2.75	Leu <sup>6</sup> NH	Leu <sup>6</sup> Hβ <sup>(R)</sup>	2.5	2.68

SC = side chain.

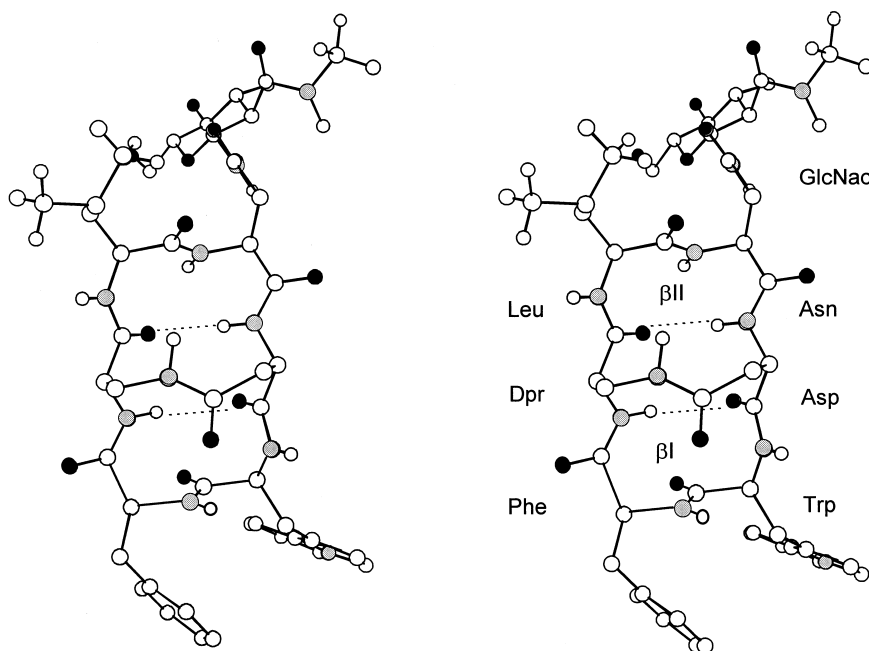


Fig. 2. Stereoplot of the  $\beta$ I,  $\beta$ II conformation of nepadutant. Oxygen atoms are indicated by filled circles, nitrogen atoms are hatched. The  $\phi$ ,  $\psi$ , and  $\chi_1$  angles of the lowest energy conformations of the peptidic moiety of nepadutant and its by-products were determined. Asn<sup>1</sup>:  $\phi = 68^\circ$ ,  $\psi = 7^\circ$ ,  $\chi_1 = \text{n.d.}$ ; Asp<sup>2</sup>:  $-140, 157, 60$ ; Trp<sup>3</sup>:  $-48, -54, 180$ ; Phe<sup>4</sup>:  $-101, 28, -60$ ; Dpr<sup>5</sup>:  $-167, -164, 60$  and Leu<sup>6</sup>:  $-75, 126, 180$ .

able in addition to the backbone conformation. Several medium range NOEs between the two ring systems are observable. These NOEs lead to a parallel arrangement of the phenyl and indolyl rings. Further confirmation was obtained by analysis of the homonuclear coupling constants  $^3J_{\text{H}\alpha\text{H}\beta}$  (Table 1). It was possible to demonstrate conclusively the predominance of the  $g_{2t_3}$  rotamer ( $\chi_1 = 180^\circ$ ) and  $t_2g_3$  rotamer ( $\chi_1 = -60^\circ$ ) for Trp<sup>3</sup> and Phe<sup>4</sup>, respectively. This result is important because the dipeptide sequence Trp–Phe is intrinsic to the drug's site of action in the binding interactions with the tachykinin NK<sub>2</sub> receptor [16].

The  $^3J_{\text{H}\alpha\text{H}\beta}$  coupling constants for Asp<sup>2</sup> and Dpr<sup>5</sup> assume low values (about 2 and 4 Hz), indicating the preference of a staggered conformation with  $\chi_1 = 60^\circ$ . This less preferred orientation of the side chains permits the additional stabilization of the two  $\beta$ -turns by the formation of further hydrogen bonds, Dpr<sup>5</sup>SCNH  $\rightarrow$  Leu<sup>6</sup>CO and Asp<sup>2</sup>SCCO  $\rightarrow$  Phe<sup>4</sup>NH ( $\Delta\delta/\Delta T$  for Dpr<sup>5</sup>SCNH 0.5 ppb K<sup>-1</sup> and Phe<sup>4</sup>NH 1.2 ppb K<sup>-1</sup>).

### 3.4. Structural analysis of the sugar moiety

Differences in the chemical shifts of the protons of amino acids have been found for the Asn<sup>1</sup>H $\beta$  protons of nepadutant and all by-products, thus supporting our assumption of different neighboring sugar moieties. This is sustained by major differences in the chemical shifts of the sugar moiety (Table 1, Fig. 3). Furthermore, remarkable differences were found for the carbohydrate C<sup>1</sup>H coupling pattern. The  $^3J(\text{C}^1\text{H}-\text{N}^1\text{H})$  coupling has been found with about 9 Hz in all cases. In contrast, values between 1 and 9 Hz were observed for the vicinal coupling  $^3J(\text{C}^1\text{H}-\text{C}^2\text{H})$  (Table 1). The uniform  $^3J(\text{C}^1\text{H}-\text{N}^1\text{H})$  couplings directed to the peptide core and the different couplings  $^3J(\text{C}^1\text{H}-\text{C}^2\text{H})$  directed to the carbohydrate structure are caused by  $\alpha$ - or  $\beta$ -glycosidic linkage and sterical differences at the C<sup>2</sup> position of the carbohydrate moiety.

In the COSY spectra, the typical spin system of a pyranose

structure was found for nepadutant, MEN11420A and MEN11420D. In contrast to these data, the spin system of the sugar moiety differs in positions  $^4\text{C}-^6\text{C}$  for MEN11420C. This spin system pattern confirms a furanose structure for MEN11420C (Fig. 3).

Structure elucidation of the sugar moieties of nepadutant and its by-products can be summarized as follows: nepadutant shows a transoid orientation of the two acetamido groups. This finding, and the intermediate temperature coefficient of the NH at C<sup>2</sup>, suggest the occurrence of a C7 H-bound  $\gamma$ -turn-like structure, and corresponds with NMR studies on a variety of *N*-glycopeptide models [17]. NMR studies on MEN11420A demonstrate the  $\beta$ -linkage of 2-acetamido-2-deoxy-D-mannopyranose on Asn<sup>1</sup>. The by-product MEN11420A is a consequence of the impurity  $\beta$ -D-mannopyranosylamine in  $\beta$ -D-glucopyranosylamine as a starting material in the last step of synthesis. For MEN11420C, investigations show the  $\beta$ -linkage of 2-acetamido-2-deoxy- $\beta$ -D-glucofuranose on Asn<sup>1</sup>. Chemical shifts and couplings of MEN11420D demonstrate the  $\alpha$ -glycosidic linkage of the sugar moiety 2-acetamido-2-deoxy-D-glucopyranose on Asn<sup>1</sup>. The by-products MEN11420C and MEN11420D are caused by the phenomenon of mutarotation during amination of 2-acetamido-2-deoxy-D-glucopyranose via an open chain intermediate and finally cyclization to  $\alpha$ -D-glucopyranosamine or  $\beta$ -D-glucofuranosamine.

We can summarize, that the by-products profile is characterized by the occurrence of two detectable mutarotation products, MEN11420C and MEN11420D, populated corresponding to the ratio of mutarotation products of *N*-acetyl glucosamine. Another type of hexose derivative would result in a different by-product profile. The by-product MEN11420A is caused by impurity 2-acetamido-2-deoxy- $\beta$ -D-mannopyranosylamine in  $\beta$ -D-GlcNAc, which is coextracted during the isolation of  $\beta$ -D-GlcNAc from chitin.

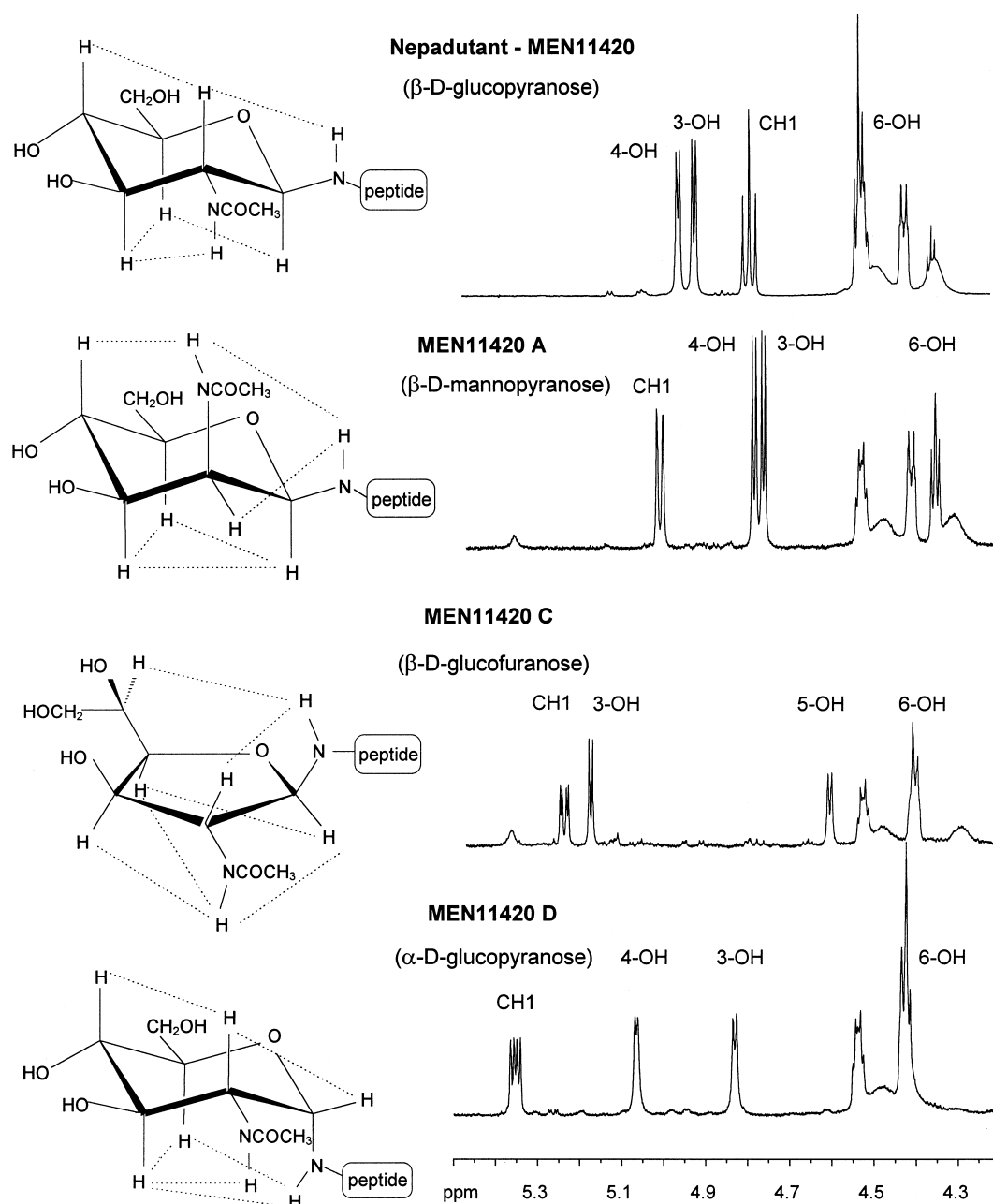


Fig. 3.  $^1\text{H}$ -NMR spectra of nepadutant and MEN11420A–D in the range of the anomer sugar protons and  $\text{H}_\alpha$  protons of the amino acids at 298 K (right). The amino acid protons are extensively masked at this temperature. The structures of the associated sugar moieties and the detected interproton distances (NOEs, dashed lines) are shown left.

#### 4. Discussion

The synthesis and conformational analysis of constrained analogues of native peptides has emerged as a very powerful approach in peptide drug design [18]. A drastic reduction of conformational space in peptide molecules is achieved by backbone cyclization. In the case of the reported new  $\text{NK}_2$  receptor antagonist nepadutant discussed here, a further reduction of the conformational space was achieved by an additional side chain–side chain linkage. This further constraint divides the peptide molecule into two parts. Each of these parts forms a  $\beta$ -turn, where the two linkage-building amino acids  $\text{Asp}^2$  and  $\text{Dpr}^5$  belong to both  $\beta$ -turns, and form the characteristic hydrogen bonds. In the homochiral cyclic hexa-

peptide unit, we found a  $\beta\text{I}$ ,  $\beta\text{II}$ -turn conformation. Here, the arrangement of the side chain–side chain bridge fixes the orientation of the amide bonds centered in the turns. Therefore, the known  $\beta\text{I}/\beta\text{II}$  flip found in many analyzed homochiral  $\beta$ -turns is not observed [19]. Interestingly, such a dynamic switch between  $\beta\text{I}/\beta\text{II}$ -turns was also observed in an glycosylated cyclic peptide near the glycosylation site [20]. The bicyclic peptide design prevents the often described  $\text{C}_2$  symmetric conformation of cyclic hexapeptides [21]. In our design the Trp–Phe sequence was exposed in well defined spatial arrangements. The formation of a hydrophobic sandwich or cluster of the indolyl and phenyl rings within the active dipeptide sequence Trp–Phe is noticeable. The homochiral hydrophobic cluster formation over a *trans* peptide bond was also observed

in other peptides [22,23]. Such a hydrophobic sandwich is conceivable as a docking site for the receptor binding.

While the conformational requirements for the biological activity are fulfilled by the bicyclic peptide design, the requirements for clinical use are not met by the pure peptide. Nepadutant has been developed due to the extremely poor water solubility of the pure peptide MEN10627. The majority of naturally occurring proteins are glycosylated, and the variety of linkages between reducing sugar and proteins is enormous [24]. The common structure of *N*-linked glycoproteins consists of a pentasaccharide core with *N*-acetylglucosamine asparagine linkage. The bicyclic glyco-hexapeptide nepadutant was synthesized accordingly by coupling of  $\beta$ -D-GlcNAc-NH<sub>2</sub> with the aspartic acid of the bicyclic peptide precursor MEN11282. NMR analyses with *N*-glycopeptides have suggested that the polypeptide and the oligosaccharide have little mutual effect on local conformations [17].

The characterization of the by-products of nepadutant show that no real contamination occurs. In fact, the natural process of mutarotation of glucose is frozen by the linkage of the glucose and peptide moiety. The process of mutarotation does not occur in the glycopeptide, in such a way as to enable us to separate and measure the single components. Although there is no way to avoid the formation of MEN11420A, -C and -D, but the by-products resulting from the mutarotation are uncritical.

This investigation indicates the continued importance of conformationally constrained antagonist molecules for the design of potent lead structures in the development of drugs. Here, the conformational rigidity increases potency, specificity and the half-life of the molecule in the living body. It can be assumed that an increase of the activity is accessible by further restrictions of the conformational space, for example by non-peptidic  $\beta$ -turn mimetics.

**Acknowledgements:** We are very grateful to Antonio Triolo (Menarini AG) for the mass spectral analysis, to Simone Berg (Berlin-Chemie AG) for racemization tests, Wolf-Dieter Bloedorn (Humboldt University Berlin) for excellent NMR spectra and to Marco Criscuoli and Carlo A. Maggi (Menarini AG) for critical reading of the manuscript.

## References

- [1] Regoli, D., Drapeau, G., Dion, S. and D'Orleans-Juste, P. (1989) *Pharmacology* 33, 1–15.
- [2] Maggi, C.A., Patacchini, R., Rovero, P. and Giachetti, A. (1993) *J. Auton. Pharmacol.* 13, 23–93.
- [3] Gao, Z.L. and Peet, N.P. (1999) *Curr. Med. Chem.* 6, 357–388.
- [4] Osakada, F., Kubo, K., Goto, K., Kanazawa, I. and Muneata, E. (1986) *Eur. J. Pharmacol.* 120, 201–208.
- [5] Maggi, C.A., Patacchini, R., Astolfi, M., Rovero, P., Giachetti, A. and Van Giersbergen, P.L.M. (1992) *Neuropeptides* 22, 93–98.
- [6] Patacchini, R., Giuliani, S., Lazzeri, M., Turini, A., Quartara, L. and Maggi, C.A. (1997) *Neuropeptides* 31, 71–77.
- [7] Pavone, V., Lombardi, A., Pedone, C., Quartara, L., Maggi, C.A. (1994) in: *Peptides: Chemistry, Structure and Biology* (Hodges, E.S. and Smith, J.A., Eds.), pp. 487–489, Escom, Leiden.
- [8] Santicoli, P., Giuliani, S., Patacchini, R., Tramontana, M. and Criscuoli, M. (1997) *Naunyn-Schmiedeberg Arch. Pharmacol.* 356, 678–688.
- [9] Catalioto, R.M., Criscuoli, M., Cucchi, P., Giachetti, A., Giannotti, D., Giuliani, S., Lecci, A., Lippi, A., Patacchini, R., Quartara, L., Renzetti, A.R., Tramontana, M., Arcamone, F. and Maggi, C.A. (1998) *Br. J. Pharmacol.* 123, 81–91.
- [10] Hänsicke, A., Caciagli, V., Cardinali, F., Liotine, T., Tuchalski, G., Maggi, C.A. and Giachetti, A. (1994) *Eur. J. Pharm. Sci.* 2, 145.
- [11] Caciagli, V., Cardinali, F., Hänsicke, A., Liotine, T., Tuchalski, G., Bonelli, F., Centini, F., Sisto, A. and Lombardi, P. (1993, publ. 1994) in: *Innovation Perspect. Solid Phase Synth. Collect. Pap., 3rd Int. Symp.* (Epton, R., Ed.), pp. 465–468, Mayflower Worldwide, Birmingham.
- [12] Bull, T.E. (1988) *J. Magn. Reson.* 80, 470–481.
- [13] Brünger, A.T., XPLOR, Version 3.1, Yale University, New Haven, CT, USA.
- [14] Gierasch, L.M., Deber, C.M., Madison, V., Niu, C.-H. and Blout, E.R. (1981) *Biochemistry* 20, 4730–4738.
- [15] Kurz, M., Schmieder, P. and Kessler, H. (1991) *Angew. Chem. Int. Ed. Engl.* 30, 1329–1331.
- [16] Giolitti, A., Cucchi, P., Renzetti, A.R., Rotondaro, L., Zappitelli, S. and Maggi, C.A. (2000) *Neuropharmacology* 39, 1422–1429.
- [17] Vass, E., Láng, E., Samu, J., Majer, Zs., Kajtár-Peredy, M., Mák, M., Radics, L. and Hollósi, M. (1998) *J. Mol. Struct.* 440, 59–71.
- [18] Hruby, V.J., Li, G.G., Haskelluevano, C. and Shenderovich, M. (1997) *Biopolymers* 43, 219–266.
- [19] Konat, R.K., Mierke, D.F. and Kessler, H. (1996) in: *Conformational Homogeneity and Solvent Effects in Cyclic Peptides* (Kau-maya, P.T.P. and Hodges, R.S., Eds.) *Peptides: Chemistry, Structure and Biology, Proc. of the 14th Am. Pept. Symp.*, June 18–23, 1995, Columbus, OH, pp. 839–840, Mayflower Scientific, Birmingham.
- [20] Gerz, M., Matter, H. and Kessler, H. (1994) *Int. J. Pept. Protein Res.* 43, 248–257.
- [21] Kopple, K.D. and Parameswaran, K.N. (1983) *Int. J. Pept. Protein Res.* 21, 269–280.
- [22] Müller, G., Gurrath, M., Kurz, M. and Kessler, H. (1993) *Proteins Struct. Funct. Genet.* 15, 235–251.
- [23] Weißhoff, H., Frost, K., Brandt, W., Henklein, P., Mügge, C. and Frömmel, C. (1995) *FEBS Lett.* 372, 203–209.
- [24] Lis, H. and Sharon, N. (1993) *Eur. J. Biochem.* 218, 1–27.